Developing Functional Relationships Between Solar Wind/Interplanetary Magnetic Field Parameters and Local Plasma Velocity on a Global-Scale Grid

Eden L. Thompson & William A. Bristow
Department of Meteorology and Atmospheric Science, Pennsylvania State University

Background

Researchers have developed empirical models to predict the ionospheric plasma convection corresponding to IMF parameters (e.g., Thomas & Shepherd, 2018; Holt et al., 1987; Ridley et al., 2000). These models convey the electrostatic potential as an expansion in global orthogonal functions. High-latitude observations such as ionospheric electric field observations (Richmond & Kamide, 1988), plasma velocity observations (Haaland et al., 2007), and magnetometer observations (Waters et al., 2001) were used to constrain the expansion. A global-scale representation can potentially miss localized variations of plasma velocity at a scale smaller than the functions used for the fitting. This research hopes to overcome the constraints of global-scale representation by developing convection models in individual latitude and local time bins.

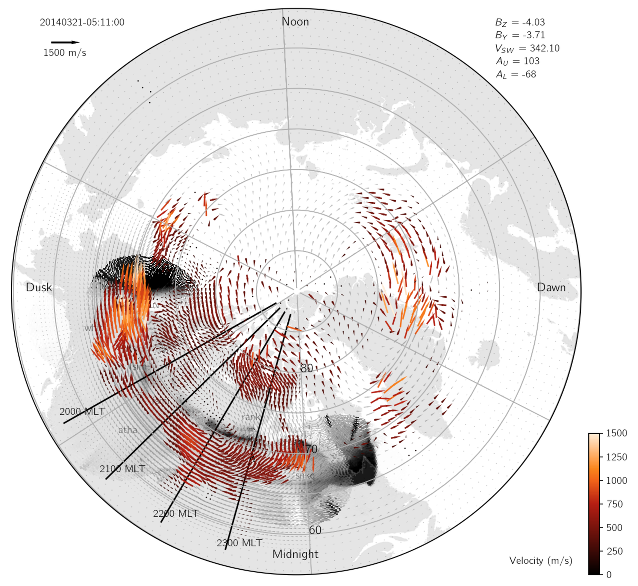

Figure 1. Example of a plasma convection pattern measurement from SuperDARN.

To conduct this research, a large number of ionospheric observations were needed. SuperDARN is a network of radars that measure the dynamics of plasma convection in the ionosphere (Greenwald, et al., 1995). By applying the Global-Local Divergence Free Fitting algorithm (Bristow, et al., 2022) to this raw data, a convection database over the years 2013-2023 was created. The different estimates were binned across a grid of all MLTs between 55° and 90° magnetic latitude. Each grid cell covered an equal amount of area, with longitude spacing varying with latitude and latitude spacing always being 1°.

In each of the grid cells, the velocity was binned against several different functions of the IMF/solar wind parameters. Through this, it was possible to investigate if a single functional relationship applies to the high-latitude ionosphere as a whole. By using a different functional dependence in each grid cell, it may be possible to better represent the convection pattern than current models.

Methods

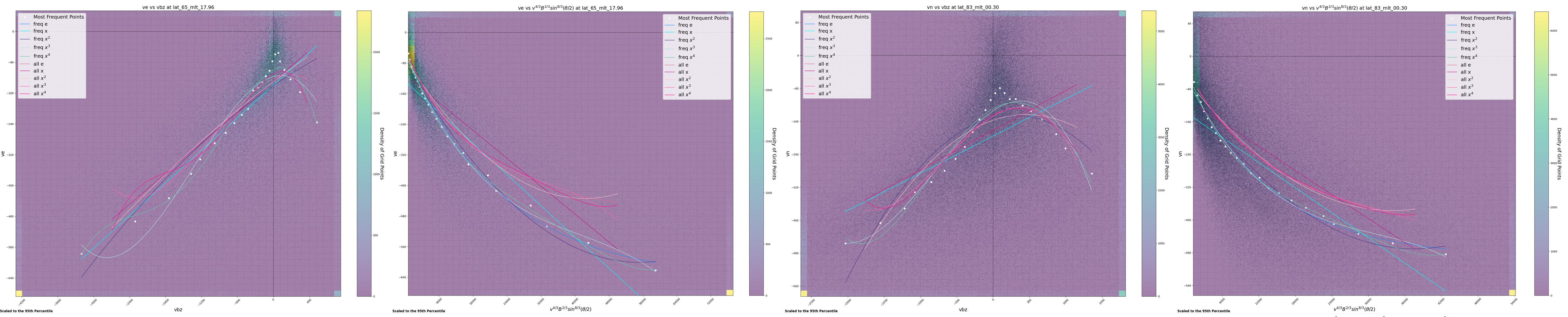

Figure 2. Scatterplots at latitude 65° MLT 17.96 and latitude 83° MLT 00.30 with the plasma velocity evaluated against the functions $v\,B_z$ and $v^{4/3}B^{2/3}\sin^{8/3}(\theta/2)$.

Scatterplots were produced to identify relationships between solar wind parameters and plasma velocity measurements. A contour was then applied to portray the areas on the scatterplot with the highest concentration of data points to comprehend which points hold the most significance. Exponential, linear, quadratic, cubic, and quartic functions were fitted to the data using the total points and the most frequent points. With this range of equations plotted on the scatterplot, a vague understanding of the strongest functional relationship was presented by the curves.

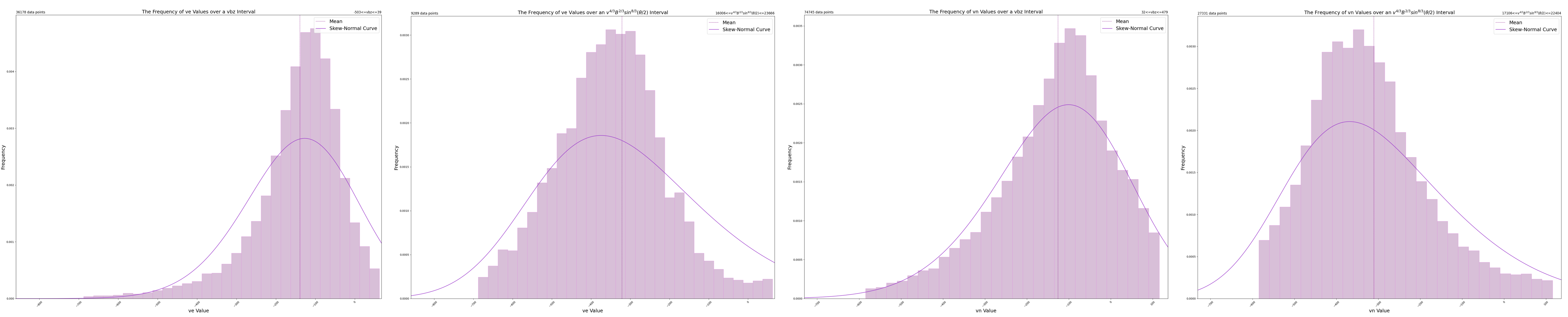

Figure 3. Histogram binned over a range at latitude 65° MLT 17.96 and latitude 83° MLT 00.30 to demonstrate where the most frequent plasma velocity value resides in comparison to the mean.

To better determine the most representative functional relationship, the residual variance of each curve was calculated. These residuals were calculated by subtracting the fitted line from the observations. Histograms were then used to display the residuals.

Results

The two locations that will be compared is the grids at latitude 65° MLT 17.96 and latitude 83° MLT 00.30. The velocity will be evaluated against the functions $v\,B_z$ and $v^{4/3}B^{2/3}\sin^{8/3}(\theta/2)$. The function to most accurately represent the relationship was determined to be whichever histogram had the lowest residual variance.

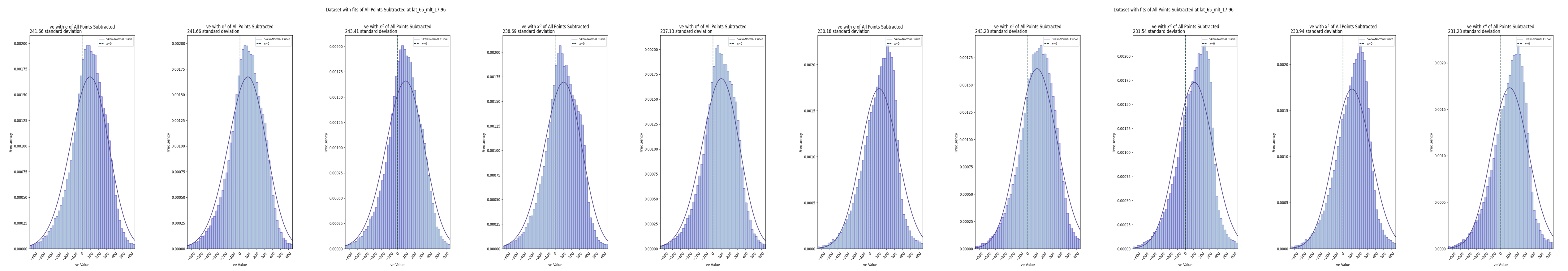

Figure 4. Histograms at latitude 65° MLT 17.96 of the east-west velocity against $v\,B_z$ and $v^{4/3}B^{2/3}\sin^{8/3}(\theta/2)$ with the fitted data subtracted from the overall data.

At latitude 65° MLT 17.96, the quartic function best represents the relationship between ve and $v\,B_z$, while the exponential function was the closest portrayal of the relationship between ve and $v^{4/3}B^{2/3}\sin^{8/3}(\theta/2)$.

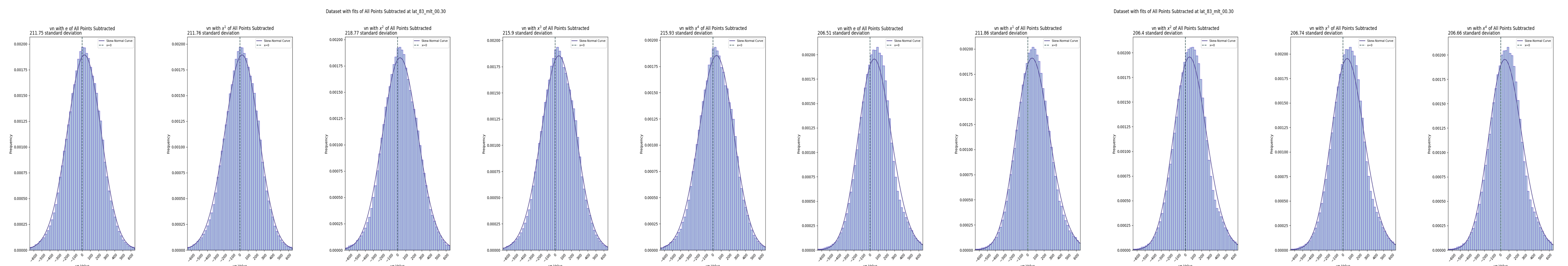

Figure 5. Histograms at latitude 83° MLT 00.30 of the north-south velocity against $v\,B_z$ and $v^{4/3}B^{2/3}\sin^{8/3}(\theta/2)$ with the fitted data subtracted from the overall data.

At 83° MLT 00.30, the linear/exponential function best represents the relationship between vn and $v\,B_z$. For the relationship between vn and $v^{4/3}B^{2/3}\sin^{8/3}(\theta/2)$, the quadratic function appears to be the strongest fit.

While this only shows a few examples, the variability of the most representative relationship was present when observing all generated plots.

The next steps for this research include examining uncertainties to properly select the most optimal model. This model will then be used to construct a plasma convection pattern to compare to existing models.

Conclusion

- The histograms indicate that the best function to represent the convection pattern is different for each of the examples used.
- This research supports the idea that analyzing on a grid provides a more accurate way to portray the convection pattern than existing models.

References

Thomas, E. G., Shepherd, S. G. (2018). Statistical patterns of ionospheric convection derived from mid-latitude, high-latitude, and polar SuperDARN HF radar observations. Journal of Geophysical Research: Space Physics, 123, 3196–3216. https://doi.org/10.1002/2018JA025280

Holt, J. M., R. H. Wand, J. V. Evans, and W. L. Oliver (1987), Empirical models for the plasma convection at high latitudes from Millstone Hill observations, J. Geophys. Res., 92(A1), 203–212, doi:10.1029/JA092iA01p00203.

Ridley, A. J., Crowley, G., Freitas, C. (2000). An empirical model of the ionospheric electric potential. Geophysical Research Letters, 27(22), 3675–3678. https://doi.org/10.1029/1999gl011161

Richmond, A. D., and Y. Kamide (1988), Mapping electrodynamic features of the high-latitude ionosphere from localized observations: Technique, J. Geophys. Res., 93(A6), 5741–5759, doi:10.1029/JA093iA06p05741.

Haaland, S. E., Paschmann, G., Förster, M., Quinn, J. M., Torbert, R. B., McIlwain, C. E., Vaith, H., Puhl-Quinn, P. A., and Kletzing, C. A.: High-latitude plasma convection from Cluster EDI measurements: method and IMF-dependence, Ann. Geophys., 25, 239–253, https://doi.org/10.5194/angeo-25-239-2007, 2007.

Waters, C. L., Anderson, B. J., Liou, K. (2001). Estimation of global field aligned currents using the Iridium® System Magnetometer Data. Geophysical Research Letters, 28(11), 2165–2168. https://doi.org/10.1029/2000gl012725

Greenwald, R. A., Baker, K. B., Dudeney, J. R., Pinnock, M., Jones, T. B., Thomas, E. C., et al. (1995). DARN/SUPERDARN: A global view of the dynamics of high-latitude convection. Space Science Reviews, 71, 761-796.

Bristow, W. Lyons, L. Nishimura, Y. Shepherd, S. Donovan, E.. (2022). High-Latitude Plasma Convection Based on SuperDARN Observations and the Locally Divergence Free Criterion. Journal of Geophysical Research: Space Physics. 127. 10.1029/2022JA030883.